

Effect of Exchange and Correlation on Calculated Properties for CO Adsorption on NiO(100)

Thomas Bredow*

Theoretische Chemie, Universität Hannover, Am Kleinen Felde 30, 30167 Hannover, Germany

Received: December 20, 2001; In Final Form: April 25, 2002

The adsorption of carbon monoxide on the NiO(100) surface has been investigated theoretically with first-principles Hartree–Fock, density functional, and hybrid methods. The surface was modeled with embedded clusters and periodic slabs that were shown to give similar results for the CO adsorption energy, adsorbate geometry, and vibration frequency. The effect of the description of the electron exchange and correlation given by the various methods on the interaction of CO and NiO has been investigated. While the inclusion of electron correlation leads to an increase of the calculated interaction energy compared to the Hartree–Fock approach and improves the agreement with experiment considerably, the role of electron exchange is less clear. Close agreement of calculated and experimental NiO/CO adsorption energies was achieved by using a density functional approach for exchange and correlation, but at the same time a large deviation of the calculated C–O frequency shift from the experimental value was obtained. This is explained by the role of exchange in the description of the substrate electronic structure. Best overall agreement for energetic and spectroscopic features was achieved by a hybrid approach that combines exact Hartree–Fock exchange with a correlation functional.

1. Introduction

Metal oxides, especially of transition metals, have attracted considerable attention in the recent past due to their potential as cost-effective catalysts and catalyst support.^{1,2} A crucial step for the understanding of chemical processes in heterogeneous catalysis is the knowledge of bonding mechanisms between adsorbed molecules and the surfaces. Theoretical calculations have provided reliable information about adsorbate geometries, bond strength, binding mechanism, and spectroscopic properties for a variety of systems.¹ In many cases little or no experimental information has been available until recently, either due to difficulties in preparing well-defined surfaces or because spectroscopic methods were inapplicable to oxide systems. This situation has changed in the last years as a result of new developments in preparation techniques and spectroscopic methods. A particular example is the adsorption of carbon monoxide on the (100) surfaces of the isostructural oxides of magnesium and nickel. For CO/MgO(100), there has been a long controversy among theorists and experimentalists about the nature and the strength of the Mg–CO interaction. Only recently, a careful experimental study by Freund et al. gave a conclusive answer to the problem,^{3,4} confirming the results of previous high-level calculations. CO is only weakly physisorbed at the regular (100) surface. A comprehensive review about the problematic of this system has been written by Pacchioni.⁵

A similar discrepancy between theory and experiment exists for the system CO/NiO and has been discussed recently.^{3,6} Earlier first-principles calculations described the CO–NiO interaction as considerably weaker than found by the recent experiments. This is documented by the Ni–CO distance, which has been measured to 2.07 Å,⁶ while calculated values range from 2.49 to 2.86 Å.^{7,8} The measured adsorption energy is 0.30 eV.^{3,4} The values of ab initio calculations range from 0.08 to 0.24 eV.^{8,9} The latter value was reported to be overestimated

because it had not been corrected by the basis set superposition error (BSSE).

The Hartree–Fock (HF) method generally underestimates the bonding interaction between CO and metal atoms on oxide surfaces, which is mainly due to dispersion effects. It is necessary to take into account electron correlation, either by exact configuration interaction (CI) methods or by approximate procedures such as perturbation theory or by using correlation functionals derived from density functional theory (DFT). Even for moderately sized surface models, the computational cost of exact CI approaches is extremely large. Therefore, the use of DFT methods has become a standard in computational studies of solids and surfaces. For many systems, good agreement between calculated and measured properties has been found in this way. Known exceptions are systems with strongly localized unpaired electrons, where DFT approaches give a too delocalized description of the open shells and can lead to qualitatively incorrect results.¹⁰ Another example where standard DFT methods especially within the local density approximation (LDA) fail to reproduce experimental results is the electronic structure of magnetic transition metal oxides, in particular the valence band structure of NiO.¹¹ Here DFT methods generally underestimate the optical band gap and also describe the contribution of Ni 3d orbitals in the highest part of the valence band in a way not corresponding to recent experimental interpretation.¹² In a recent study, a comparison between HF, GGA-DFT, and hybrid methods for the calculation of MgO, NiO, and CoO bulk properties has been performed.¹³ It has been found that hybrid methods where the exact HF exchange is combined with DFT correlation give best agreement with experimental literature data for properties of transition metal oxides, especially for NiO.

In the present study the effect of the electron correlation and exchange on the adsorption properties of CO on the NiO(100) surface is investigated by a similar comparison of methods as in the previous study.¹³

* E-mail: bredow@mbbox.theochem.uni-hannover.de

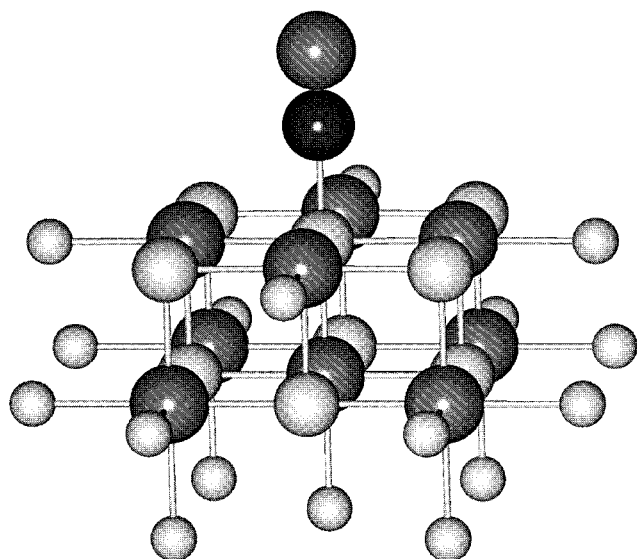


Figure 1. Ni_9O_9 cluster used to model the $\text{NiO}(100)$ surface together with adsorbed CO and the 17 Ca model ions used for embedding; the surrounding 865 point charges are not shown: gray spheres, Ni; large dark spheres, O; black sphere, C; small gray spheres, Ca.

2. Models and Computational Methods

Two models were employed to represent the $\text{NiO}(100)$ surface, a Ni_9O_9 cluster (Figure 1) and a periodic slab. The cluster was embedded in a finite field of point charges (PCs), to take into account long-range electrostatic interactions from the Madelung field of the surface. The PCs were arranged in a $15 \times 15 \times 4$ configuration. The central $3 \times 3 \times 2$ PCs were replaced by Ni and O atoms and were treated quantum chemically. Since for solids with rock-salt structure like MgO and NiO the Madelung sum is rapidly converging with increasing distance,¹⁵ this simple embedding procedure is expected to provide a good approximation to the surface electrostatic potential, at least for the central position of the cluster, as shown previously.¹⁶ A detailed discussion of the effect of embedding on calculated properties for the CO–MgO system can be found in ref 17. However, embedding in point charges leads to artificial polarization, especially of the anions at the cluster boundary.¹⁸ To avoid this effect, the 17 PCs representing Ni atoms closest to the cluster were replaced by total ion potentials (TIPs). In the present case, the TIPs consist of the $\text{Ca}^{2+}[1s-3p]$ effective core potential.¹⁹ The Ca^{2+} TIP was taken rather than the Ni^{2+} TIP for computational convenience and because it has been successfully used in a previous study of the $\text{TiO}_2(110)$ surface.²⁰ The Ni_9O_9 cluster was calculated with a multiplicity of 19. This corresponds to a ferromagnetic state of NiO where each nickel is formally Ni^{2+} with a $^3\text{B}_2$ ground state (local C_{4v} symmetry). The ground state of solid NiO is antiferromagnetic AF_2 with parallel spins along the (111) planes,²¹ but the energetic difference between the ferromagnetic and the antiferromagnetic state is within a few kJ/mol, and it is assumed that magnetic coupling between the Ni atoms does not play an important role in the CO adsorption process.

The calculations were performed using the spin polarized, unrestricted method. This approach generally does not give pure spin states, and the resulting energy may be too low due to spin contamination. However, in the present calculations the expectation value of the \hat{S}^2 operator was always within 0.02 of the nominal value. It is therefore expected that the energetic error is small.

The slab model consists of three layers, each containing four NiO units. Here the antiferromagnetic AF_2 ground state of bulk NiO was assumed for the model. One CO molecule was adsorbed on each side of the repeat unit. The resulting CO coverage θ was 0.25 with a minimal CO–CO distance of 5.87 Å.

The experimental Ni–O distance of 2.08 Å²² was assumed for both cluster and slab models. No optimization of the lattice atoms after CO adsorption was performed. Two different surface geometries were considered in the cluster calculations corresponding to the unrelaxed and relaxed $\text{NiO}(100)$ surface prior to adsorption. The geometry parameters of the relaxed surface were obtained by periodic slab calculations. In the slab calculations of the CO/NiO system, only the relaxed $\text{NiO}(100)$ surface structure was used. The CO molecule was set perpendicular to the $\text{NiO}(100)$ surface with the C atom pointing toward a surface Ni atom; see Figure 1. The slight deviations from the perpendicular arrangement as found in recent experiments⁶ were not taken into account.

In all calculations, the carbon and oxygen atoms of CO were described with a standard 6-311+G(d,p) basis set.²³ For the Ni and O atoms of nickel oxide, different basis sets were used in the cluster and in the slab calculations. The cluster calculations were performed with the Gaussian94 program package.²⁴ The cluster Ni basis [14s9p5d/9s5p3d], abbreviated as 6-311G, was augmented with diffuse p- and d-shells with exponents 0.2242 and 0.1622, respectively (“6-311G+p,d”). The cluster O atoms were described with the same 6-311+G(d,p) basis set as the oxygen of CO.

For the slab calculations, the crystalline-orbital program CRYSTAL98 was used.²⁵ The atom-centered basis sets used to build up the Bloch functions were 8-6411G41d (Ni) and 8-411G1d (O) for NiO.²⁶ These basis sets have been optimized for NiO in previous CRYSTAL studies.²¹ For comparison, the same Ni and O basis sets were also used in a cluster calculation. For that cluster calculation the CRYSTAL basis sets were augmented with diffuse sp and d shells in order to minimize the BSSE. The exponents of the diffuse functions were chosen to be one-third of the smallest from the standard basis. The resulting cluster basis sets were 8-64111G411d (Ni) and 8-4111G11d (O). For CO the same 6-311+G(d,p) basis set as in the cluster calculations was used, except that the most diffuse sp shell of the C basis had to be removed in order to avoid linear dependencies in the periodic calculations.

Four different standard methods were used for the calculation of adsorption properties of CO/NiO(100): (a) the Hartree–Fock (HF) method; (b) a hybrid method where the exact HF exchange is combined with the Lee–Yang–Parr (LYP) correlation functional,²⁷ HFLYP; (c) the B3LYP three-parameter hybrid method;²⁸ and (d) the pure DFT method BLYP.²⁹ In this way the same expression for the correlation energy, the LYP functional, was combined with three different expressions for the electron exchange with a decreasing amount of the exact HF exchange: 100% in HFLYP, 20% in B3LYP, and 0% in BLYP. The effect of the different description of exchange and correlation on the adsorption properties of CO at NiO(100) will be described in the next section.

3. Results and Discussion

The calculated results for CO adsorption at the $\text{NiO}(100)$ surface are summarized in Table 1. In particular, the optimized Ni–CO distance, $R_e(\text{Ni}-\text{C})$; the frequency for the Ni–CO stretching, $\omega_e(\text{Ni}-\text{CO})$; the dissociation energies without, D_e , and with, $D_e(\text{BSSE})$, BSSE correction; the C–O equilibrium

TABLE 1: Calculated Adsorption Properties for CO/NiO(100): Ni–C Equilibrium Distance, $R_e(\text{Ni–C})$ (Å); Vibrational Frequency, $\omega_e(\text{Ni–CO})$ (cm^{-1}); Dissociation Energy, D_e ; BSSE-Corrected Value, $D_e(\text{BSSE})$ (eV); C–O Equilibrium Distance, $R_e(\text{C–O})$; Change with Respect to Gas Phase CO, ΔR (Å); C–O Vibrational Frequency, $\omega_e(\text{C–O})$; Change with Respect to Gas Phase CO, $\Delta\omega_e$ (cm^{-1}); and Change of the Dynamic Dipole Moment with Respect to Gas Phase CO, $\Delta(d\mu/dR_{\text{C–O}})$ (au)

method	model	$R_e(\text{Ni–C})$	$\omega_e(\text{Ni–CO})$	D_e	$D_e(\text{BSSE})$	$R_e(\text{C–O})/\Delta R$	$\omega_e(\text{C–O})/\Delta\omega_e$	$\Delta(d\mu/dR_{\text{C–O}})$
HF	$3 \times 3 \times 2$ cluster	2.92	76	0.15	0.00	1.105/ ± 0	2433/0	−0.07
HFLYP	$3 \times 3 \times 2$ cluster	2.38	113	0.22	0.15	1.098/+0.001	2479/−10	−0.27
HFLYP ^d	$3 \times 3 \times 2$ cluster	2.40	112	0.21	0.19	1.098/+0.001	2479/−10	
HFLYP	2×2 supercell $\theta = 0.25$	2.40	184	0.29	0.17	1.095/−0.002	2487/−3	
B3LYP	$3 \times 3 \times 2$ cluster	2.10	159	0.12	0.02	1.134/+0.006	2139/−73	−0.89
BLYP	$3 \times 3 \times 2$ cluster	1.87	306	0.33	0.23	1.161/+0.021	1941/−172	−1.43
expl		2.07 ± 0.02^a			0.30^b	$1.15(+0.10/−0.08)^d$	$2152/+9^c$	

^a Reference 6. ^b Reference 3. ^c $\nu_0/\Delta\nu_0$; ref 14. ^d Obtained with a different basis set; see the text

distance, $R_e(\text{C–O})$; the C–O vibrational frequency, $\omega_e(\text{C–O})$; and the change of the dynamic dipole moment³⁰ with respect to gas-phase CO, $\Delta(d\mu/dR_{\text{C–O}})$, have been considered and compared to experimental values from the literature where possible. The dissociation energy is the energy difference between the separated systems and the CO/NiO system. The counterpoise scheme³¹ has been applied for an estimate of the BSSE. The vibration frequency $\omega_e(\text{C–O})$ and the dynamic dipole moment $d\mu/dR_{\text{C–O}}$ have been obtained numerically. The total energy and dipole moment at five different C–O distances with fixed center of mass were calculated and fitted with fourth-degree polynomials.

The HF method only gives a weak interaction that is essentially an artifact of the basis set superposition. This can be seen from $D_e(\text{BSSE})$, which is zero, from the large Ni–C distance, and from the small Ni–CO stretching frequency (Table 1). The importance of electron correlation for the strength of the CO–surface interaction is demonstrated by a comparison of HF and HFLYP results. With HFLYP the Ni–C distance is considerably smaller, 2.38 Å, compared to 2.92 Å obtained with HF. The HFLYP desorption energy is 0.22 eV (BSSE-corrected value: 0.15 eV), not too far from the experimental value of 0.30 eV.^{3,4} At the HFLYP level the C–O distance of the adsorbed molecule remains almost unchanged with respect to the gas-phase structure. The calculated shift of the C–O stretching frequency due to the interaction with NiO is −10 cm^{-1} . The small absolute value is in agreement with the results of an experimental FTIR investigation of CO adsorption on sintered NiO.¹⁴ In the zero-coverage limit the measured value for $\nu_0(\text{C–O})$ was 2152 cm^{-1} .¹⁴ The absolute value corresponds to a frequency shift of +9 cm^{-1} with respect to the experimental gas-phase value ($\nu_0 = 2143.2 \text{ cm}^{-1}$ ³²). For the comparison of calculated ω_e and measured ν_0 shifts, it has been assumed that the anharmonic correction ω_{ex} does not change significantly due to adsorption. This correction is 13.3 cm^{-1} in the gas phase³³ but has not been determined in the adsorption experiments.¹⁴ Since the interaction between CO and the surface is weak, it can be expected that the error caused by this assumption is in the order of a few wavenumbers.

Very similar results are obtained with the supercell model at the HFLYP level (Table 1). The small coverage ($\theta = 0.25$) ensures that the lateral interaction between the adsorbate molecules is small. This was tested by comparing the energy of a periodic CO arrangement similar to that of the adsorption study, but without NiO, and a free CO molecule at the same level of theory. The energy difference was only 0.003 eV/CO, indicating that the coverage was chosen small enough to allow for a comparison with cluster calculations. With the slab model, a slightly larger Ni–CO distance is obtained, 2.40 Å, compared to the cluster model, 2.38 Å, and a $D_e(\text{BSSE})$ of 0.17 eV is calculated, only 0.02 eV larger than for the cluster model. Also, the C–O distances and the stretching frequencies of both models

are in close agreement. The deviations are 0.003 Å and 7 cm^{-1} , respectively. In the two sets of calculations, different basis sets were used. The good agreement between cluster and slab results could in principle be due to fortuitous cancellation effects. Therefore, the UHFLYP cluster results were repeated with basis sets similar to the slab model, as described in the previous section (8-641111G411d for Ni and 8-4111G11d for O). The results for this basis set are close to both the cluster calculation with the smaller basis set and the periodic calculation (Table 1). The vibrational frequencies $\omega_e(\text{Ni–CO})$ and $\omega_e(\text{C–O})$, the adsorption energy without BSSE correction D_e , and the C–O distance $R_e(\text{C–O})$ of the two cluster calculations are almost indistinguishable. The larger cluster basis (8-641111G411d/8-4111G11d) has a smaller BSSE so that $D_e(\text{BSSE})$ becomes 0.19 eV, 0.04 eV larger than for the cluster with smaller basis sets (6-311G+p,d/6-311+G(d,p)) and only 0.02 eV larger than the corresponding value of the slab model calculation.

Two conclusions can be drawn from these results. First, the TIP/PC embedded cluster model provides an accurate description of the NiO(100) surface, at least at the central position. Second, the basis sets used in the present study are large and flexible enough that a further increase can be expected not lead to significant changes. Both points will be studied in greater detail in subsections 3.2 and 3.3.

The effect of the description of electron exchange on the calculated adsorption properties was examined by employing the two popular DFT methods, B3LYP and BLYP (Table 1). With B3LYP, a much shorter Ni–CO bond, $R_e(\text{C–O}) = 2.10$ Å, is obtained compared to the result of the HFLYP method, 2.38 Å. The B3LYP result is in fact very close to the experimental distance, 2.07 ± 0.02 Å.⁶ The CO–surface vibrational frequency $\omega_e(\text{Ni–CO})$ is larger at the B3LYP level, 159 cm^{-1} , than at the HFLYP level, 113 cm^{-1} . It is therefore surprising that the interaction energy computed at the B3LYP level is smaller than at the HFLYP level and is even almost canceled by the counterpoise correction ($D_e(\text{BSSE}) = 0.02$ eV, Table 1). A possible explanation is that dispersion forces that contribute to the CO–NiO interaction are underestimated with B3LYP. This has been found in a similar study of CO adsorption on the MgO(001) surface.³⁴

A strong negative shift of the C–O vibrational frequency is obtained with B3LYP, $\Delta\omega_e(\text{C–O}) = -73 \text{ cm}^{-1}$. The absolute shift is significantly larger than the experimental value of +9 cm^{-1} .

A strong interaction of CO with the NiO surface is obtained with the BLYP method. The Ni–CO distance computed at the BLYP level, 1.87 Å, is 0.2 Å shorter than the experimental value. The strong Ni–CO interaction is documented by the surface vibrational frequency $\omega_e(\text{Ni–CO})$, 306 cm^{-1} , which is 2–3 times larger than the corresponding values at the B3LYP and HFLYP levels. A BSSE-corrected interaction energy of 0.23 eV is obtained, slightly closer to experiment than the HFLYP

values and in much better agreement compared to B3LYP. The adsorbed CO molecule has a noticeably larger C–O distance compared to the gas phase, $\Delta R_e(\text{C–O}) = 0.02 \text{ \AA}$, and shows a pronounced shift of the C–O stretching frequency, $\Delta\omega_e(\text{C–O}) = -172 \text{ cm}^{-1}$. This is much larger than experimentally observed. This discrepancy makes a closer examination of DFT results for the CO/NiO system necessary. In a previous study¹³ of electronic properties of bulk NiO it has been found that GGA-DFT methods such as BLYP overestimate the contribution of the Ni 3d levels to the uppermost part of the NiO valence band with respect to experimental interpretations.¹² In other words, the BLYP Ni 3d levels of NiO are too high in energy. At the HFLYP level, the highest occupied levels of the NiO valence band are dominated by O 2p orbitals and the Ni 3d levels are at lower energies. The B3LYP method gives an intermediate description with a mixture of O 2p and Ni 3d near the valence band edge.¹³

The covalent part of the CO–metal interaction involves a balance of σ and π contributions.³⁵ It has been analyzed for many cases, e.g. with the constrained space orbital variation (CSOV) method.³⁶ Unfortunately, the CSOV analysis is not implemented in the codes employed in this study. Alternatively, the dynamic dipole moment $d\mu/dR_{\text{C–O}}$ has been considered. The CO-to-metal- σ contribution increases $d\mu/dR_{\text{C–O}}$ while the metal-to-CO- π contribution decreases the dynamic dipole moment.³⁰ It can be expected that electron transfer from Ni to CO is facilitated when the energy of occupied Ni 3d levels in the NiO surface increases, as occurs in the sequence HFLYP–B3LYP–BLYP. The consequence would be a decrease of $d\mu/dR_{\text{C–O}}$ and an increase of the covalent interaction. The remaining contributions to the CO/NiO interaction, namely the Pauli repulsion, electrostatic interaction, and polarization effects, will not be included in the present discussion. The dynamic dipole moment of the system CO/Ni₉O₉/TIP/PC has been calculated for the methods HF, HFLYP, B3LYP, and BLYP. In Table 1, the differences with respect to gas-phase CO at the same levels of theory are presented. At the HF level the change $\Delta(d\mu/dR)$ is close to zero, in correspondence with the negligible interaction energy. With decreasing HF contribution to the exchange expression in the sequence HFLYP–B3LYP–BLYP, the change of the dynamic dipole moment becomes more negative. This is an indication for an increase of the charge transfer from Ni to CO, in agreement with the above considerations. In previous CSOV analyses of the CO interaction with metal oxide surfaces (e.g. for the CO/Cu₂O system³⁷), it has been shown that the metal \rightarrow CO donation is responsible for a negative shift of $\omega_e(\text{C–O})$. The same effect is observed here when the methods HFLYP, B3LYP, and BLYP are compared. At the same time the interaction energy should increase. This is the case for HFLYP and BLYP. It remains, however, unclear why the B3LYP method gives a smaller interaction energy than HFLYP, both with and without counterpoise correction.

From a comparison of experimental and calculated C–O frequency shifts at the B3LYP and BLYP levels, it is concluded that the Ni-to-CO- π donation obtained with these methods is too strong. This artifact is connected with the description of the NiO electronic structure at the same levels of theory. Therefore, although the BLYP approach gives a very good agreement with experiment for the CO/NiO interaction energy, it does not properly describe the physical process of the adsorption. This failure demonstrates the importance of an exact treatment of electron exchange for magnetic transition metal oxides where unpaired electrons are highly localized at the transition metal ions. In this respect the HFLYP hybrid approach

TABLE 2: Effect of Ni Basis Set Variation on the Calculated CO/NiO Interaction Energy: Dissociation Energy, D_e ; BSSE-Corrected Value, $D_e(\text{BSSE})$ (eV); Change of the C–O Vibrational Frequency with Respect to Gas Phase CO, $\Delta\omega_e(\text{C–O})$ (cm^{-1})

method	Ni basis	D_e	$D_e(\text{BSSE})$	$\Delta\omega_e(\text{C–O})$
HFLYP	6-311G	0.29	0.12	–4
	6-311G+p,d	0.22	0.15	–10
	6-311G+f	0.29	0.12	–4
B3LYP	6-311G	0.41	0.00	
	6-311G+p,d	0.12	0.02	
	6-311G+f	0.41	0.00	
BLYP	6-311G	0.79	0.25	
	6-311G+p,d	0.33	0.23	
	6-311G+f	0.79	0.25	

appears more appropriate, since it gives a qualitatively correct description of the electronic structure of the substrate. The agreement of the calculated interaction energy with experiment is reasonable. Unfortunately, the HFLYP method considerably overestimates the experimental Ni–CO bond length. The C–O frequency shift is small but of opposite sign compared to experiment. This is probably due to the approximate nature of the correlation treatment by employing a density functional based on a single-determinant HF wave function. The case of CO physisorption represents a rather simple case where the one-determinant approximation can be expected to be reasonable. This is no longer the case when strong covalent bonds are formed between the adsorbate and the open-shell Ni atoms at the NiO surface, which lead to a pairing of electrons. An example is the NO adsorption, which is the subject of a parallel study.³⁸

3.1. Comparison with Semiempirical Methods. The present results of first-principles methods may be compared with those of the semiempirical method MSINDO that has been recently parametrized for transition metal compounds.³⁹ In fact, the present study has been stimulated by a preliminary result obtained with the semiempirical method, where it was found that the adsorbed CO was slightly tilted with respect to the surface normal. Since at that time no experimental information on the adsorbate structure was available, it was intended to create a reliable reference by performing high-level calculations. The MSINDO results are 2.27 \AA for $R_e(\text{Ni–C})$ (with a tilting angle Θ of 2°), 0.25 eV for D_e , and $+40 \text{ cm}^{-1}$ for $\Delta\omega_e(\text{C–O})$. These results compare relatively well with the experimental data, 2.07 \AA , $12 \pm 12^\circ$, 0.30 eV , and $+9 \text{ cm}^{-1}$,^{3,6,14} at least in comparison with some of the first-principles methods reported above. For the calculation of CO adsorption, the standard parameters optimized for gas-phase molecules³⁹ were used without readjustment. This comparison shows that well-parametrized semiempirical methods are able to reproduce qualitatively and even semiquantitatively experimental results that are difficult to obtain even with high-level methods.

3.2. Basis Set Dependence. The effect of an extension of the Ni basis on the calculated CO–NiO interaction energy has been examined for three methods, HFLYP, B3LYP and BLYP (Table 2). The same embedded cluster model as before was used. It was assumed that the O basis of the NiO cluster is less important for the adsorption energy, since the oxygen atoms are not directly connected to CO. On the other hand, the 6-311+G(p,d) basis set for CO already contains diffuse and polarization functions so that further extension seemed unnecessary. In a first step the 6-311G standard Ni basis was augmented with one diffuse p and one diffuse d primitive Gaussian with exponents 0.2242 and 0.1622, respectively. In a preliminary calculation of the Ni(2+)–CO complex at the B3LYP level,

TABLE 3: Effect of PC Value and Surface Geometry Variation on Calculated CO Adsorption Properties at the BLYP Level: Change in $R_e(\text{C-O})$ with Respect to Gas Phase CO, $\Delta R_e(\text{C-O})$ (Å); BSSE-Corrected Dissociation Energy, $D_e(\text{BSSE})$ (eV); Change in C–O Vibrational Frequency with Respect to Gas Phase CO, $\Delta\omega_e(\text{C-O})$ (cm^{-1})

surface geometry	PC values	$\Delta R_e(\text{C-O})$	$D_e(\text{BSSE})$	$\Delta\omega_e(\text{C-O})$
unrelaxed	± 2.0	+0.021	0.25	−172
unrelaxed	± 1.0	+0.022	0.27	−179
relaxed	± 2.0	+0.020	0.21	−172

this procedure led to an increase of the dissociation energy by more than 0.2 eV. In contrast, the effect of the same basis set augmentation on the interaction energy between CO and the Ni_9O_9 cluster is mainly a reduction of the BSSE. The counterpoise correction decreases for all three methods, being most pronounced in the case of BLYP, where it changes from 0.54 eV (6-311G) to 0.10 eV (6-311G+p,d) (Table 2). The BSSE correction with the more extended basis set 6-311G+p,d is almost the same for the three methods. The interaction energy, however, remains almost unchanged after the basis set extension. The changes are between 0.02 and 0.03 eV. In the case of the HFLYP method, also the basis set dependence of the C–O frequency shift has been investigated (Table 2). There is only a small difference of 6 cm^{-1} between 6-311G and 6-311G+p,d. These results are in correspondence with the similarity of the adsorption results for the two basis sets 6-311G+p,d and 8-641111G411d, as mentioned in section 3. The two facts together suggest that the basis sets used are close to convergence for the properties of interest. The addition of an f polarization function had a negligible effect on the interaction energy and the C–O frequency (Table 2). Polarization functions have therefore not been used for the final calculations reported in Table 1.

3.3. Effect of Cluster Embedding and Surface Structure.

The description of long-range Coulomb interactions caused by the Madelung field of ionic compounds is generally a problem for finite cluster models. In the present study a very simple embedding procedure has been employed where the cluster is surrounded by a finite array of PCs and TIPs as described in section 2. It has already been shown in section 3 that this simple embedded cluster model gives adsorption properties in close agreement with periodic models that take full account of the Madelung field. Nevertheless, the dependence of selected properties from the embedding has been tested. A crucial parameter is the value that is given to the PCs. It has been shown⁴⁰ that the use of Mulliken charges of the corresponding cluster atoms is in some cases inadequate to fit the electrostatic potential obtained from periodic calculations. To investigate the effect of the embedding in the present study, the PCs were changed from the nominal values, ± 2 to ± 1 (in this calculation the Ca ECPs were replaced by K ECPs). The BLYP method was chosen for the comparison, since it gives the largest interaction energy so that any effect might easily be seen on the value of D_e . At the same time the average Mulliken charges computed at the BLYP level show the largest deviation from the nominal values and it might be questioned if ± 2 PCs are indeed adequate. An attempt to omit the embedding completely failed due to SCF convergence problems. A comparison of the results shown in Table 3 clearly demonstrates that the embedding has only a small influence on the Ni–CO distance, the dissociation energy D_e , and the C–O frequency shift $\Delta\omega_e(\text{C-O})$ with changes of 0.001 Å , 0.02 eV , and 7 cm^{-1} . The small dependence of the adsorption properties from the surrounding

is a consequence of the rapid convergence of the Madelung field in the highly symmetric rocksalt structure, as shown by Wolf¹⁵ and others.

The atoms on the NiO(100) surface occupy slightly different positions from their regular positions in the bulk.²¹ To investigate the effect of NiO(100) surface relaxation and rumpling on the CO adsorption, the positions of the first-layer atoms were optimized using the $2 \times 2 \times 3$ slab model that was employed for the adsorption study. With the UHFLYP method a small distortion was found, the Ni ions moving inward by 0.009 Å and the O atoms outward by 0.005 Å . These structural parameters were used in a subsequent (± 2 PC) embedded cluster calculation for CO adsorption at BLYP level (Table 2). The binding energy of CO to the relaxed NiO surface is slightly reduced compared to the unrelaxed one, by 0.04 eV , probably due to an increased Pauli repulsion between CO and the protruding O ions. This deviation is one of the error limits included in the present study. Another factor omitted presently is the rerelease of the surface due to CO binding to surface Ni atoms. This will increase D_e , but this effect is expected to be small, probably on the same order of magnitude as the relaxation effect.

4. Conclusions

The effect of the theoretical treatment of electron correlation and exchange for the description of the CO interaction with the metal atoms of the NiO(100) surface has been investigated using embedded cluster and periodic slab models. The adequacy of the cluster model for representing the surface has been demonstrated by the small influence of variations in embedding and cluster structure on the calculated properties and by the close correspondence of cluster and periodic results. It has been shown that the inclusion of electron correlation is essential for the description of the interaction between CO and Ni. In the present case, where the interaction is weak and no strong covalent bonds are formed between the adsorbate and the surface, an approximate treatment of correlation by density functionals is sufficient to describe the adsorption properties with reasonable accuracy compared with experiment. On the other hand, the description of the electronic structure of the substrate has a substantial effect on the CO–NiO interaction. The popular standard density-functional methods such as B3LYP and BLYP give too high-lying 3d states of the nickel metal in the valence band structure of NiO. As a consequence, the charge transfer from the metal to CO is overestimated if these methods are used, resulting in a too negative C–O frequency shift compared to experiment. The relatively strong interaction of CO with NiO found at the BLYP level must therefore be considered as an artifact of the method's inherent self-interaction due to the approximate nature of the exchange functional. If the exact Hartree–Fock expression for the exchange is combined with an approximation of electron correlation provided by the LYP functional, reasonable agreement is obtained between most calculated and measured adsorption properties.

Acknowledgment. I wish to thank Prof. Pacchioni for many valuable discussions. The calculations were performed on the Siemens-Fujitsu VPP300 computer system at Universität Hannover.

References and Notes

- (1) Woodruff, D. P. (Ed.) *The Chemical Physics of Solid Surfaces-Oxide Surfaces*; Elsevier: Amsterdam, 2001; Vol. 9.
- (2) Henrich, V. E.; Cox, P. A. *The Surface Science of Metal Oxides*; Cambridge University Press: Cambridge, 1996.

- (3) Wichtendahl, R.; Rodriguez-Rodrigo, M.; Härtel, U.; Kuhlenbeck, H.; Freund, H.-J. *Surf. Sci.* **1999**, 423, 90.
- (4) Wichtendahl, R.; Rodriguez-Rodrigo, M.; Härtel, U.; Kuhlenbeck, H.; Freund, H.-J. *Phys. Stat. Sol. (a)* **1999**, 173, 93.
- (5) Pacchioni, G. *Surf. Rev. Lett.* **2000**, 7, 277.
- (6) Hoefl, J.-T.; Kittel, M.; Polcik, M.; Bao, S.; Toomes, R. L.; Kang, J.-H.; Woodruff, D. P.; Pascal, M.; Lamont, C. L. A. *Phys. Rev. Lett.* **2001**, 87, 086101.
- (7) Pacchioni, G.; Cogliandro, G.; Bagus, P. S. *Surf. Sci.* **1991**, 255, 344.
- (8) Pöhlchen, M.; Staemmler, V. *J. Chem. Phys.* **1992**, 97, 2583.
- (9) Pacchioni, G.; Bagus, P. S.; in Freund, H.-J., Umbach, E. (Eds.) *Adsorption on Ordered Surfaces of Ionic Solids and Thin Films*; Springer-Verlag: Berlin, 1993; p 180.
- (10) Pacchioni, G.; Frigoli, F.; Ricci, D.; Weil, J. A. *Phys. Rev. B* **2001**, 63, 054102.
- (11) Harrison, N. M.; Saunders, V. R.; Dovesi, R.; Mackrodt, W. C. *Philos. Trans. R. Soc. London, Ser. A* **1998**, 356, 75.
- (12) Hüfner, S. *Photoelectron Spectroscopy*, 2nd ed.; Springer Series in Solid-State Sciences 82; Cardona, M., Ed.; Springer: Berlin, 1996; pp 186.
- (13) Bredow, T.; Gerson, A. R. *Phys. Rev. B* **2000**, 61, 5194.
- (14) Platero, E. E.; Scarano, D.; Zecchina, A.; Meneghini, G.; de Franceschi, R. *Surf. Sci.* **1996**, 350, 113.
- (15) Wolf, D.; Koblinski, P.; Phillpot, S. R.; Eggebrecht, J. *J. Chem. Phys.* **1999**, 110, 8254.
- (16) Pacchioni, G.; Ferrari, A. M.; Marquez, A. M.; Illas, F. J. *Comput. Chem.* **1997**, 18, 617.
- (17) Pelmenchikov, A. G.; Morosi, G.; Gamba, A.; Coluccia, S. J. *Phys. Chem.* **1995**, 99, 15018.
- (18) Nygren, M. A.; Pettersson, L. G. M.; Barandiarán, Z.; Seijo, L. *J. Chem. Phys.* **1994**, 100, 2010.
- (19) Hay, P. J.; Wadt, W. R. J. *J. Chem. Phys.* **1985**, 82, 299.
- (20) Bredow, T.; Pacchioni, G. *Surf. Sci.* **1999**, 426, 106.
- (21) Towler, M. D.; Allan, N. L.; Harrison, N. M.; Saunders, V. R.; Mackrodt, W. C.; Aprá, E. *Phys. Rev. B* **1994**, 50, 5041.
- (22) Lide, D. R. *CRC Handbook of Chemistry and Physics*, 79th ed.; CRC Press: Boca Raton, FL, 1998/1999.
- (23) Extensible Computational Chemistry Environment Basis Set Database, Version 1/29/01 <http://www.emsl.pnl.gov:2080/forms/basisform.html>.
- (24) Frisch, M. J.; Trucks, G. W.; Schlegel, H. B.; Gill, P. M. W.; Johnson, B. G.; Robb, M. A.; Cheeseman, J. R.; Keith, T.; Petersson, G. A.; Montgomery, J. A.; Raghavachari, K.; Al-Laham, M. A.; Zakrzewski, V. G.; Ortiz, J. V.; Foresman, J. B.; Cioslowski, J.; Stefanov, B. B.; Nanayakkara, A.; Challacombe, M.; Peng, C. Y.; Ayala, P. Y.; Chen, W.; Wong, M. W.; Andres, J. L.; Replogle, E. S.; Gomperts, R.; Martin, R. L.; Fox, D. J.; Binkley, J. S.; Defrees, D. J.; Baker, J.; Stewart, J. P.; Head-Gordon, M.; Gonzalez, C.; Pople, J. A. *Gaussian 94, Revision D.2*, Gaussian, Inc.: Pittsburgh, PA, 1995.
- (25) Saunders, V. R.; Dovesi, R.; Roetti, C.; Causà, M.; Harrison, N. M.; Orlando, R.; Zicovich-Wilson, C. M. *CRYSTAL98 Users Manual*, University of Torino: Torino, 1998.
- (26) http://www.ch.unito.it/ifm/teorica/Basis_Sets/mendel.html.
- (27) Lee, C.; Yang, W.; Parr, R. G. *Phys. Rev. B* **1988**, 37, 785.
- (28) Becke, A. D. *J. Chem. Phys.* **1993**, 98, 5648.
- (29) Becke, A. D. *Phys. Rev. A* **1988**, 38, 3098.
- (30) Hermann, K.; Bagus, P. S.; Bauschlicher, C. W., Jr. *Phys. Rev. B* **1984**, 30, 7313.
- (31) Boys, S. F.; Bernardi, F. *Mol. Phys.* **1970**, 19, 553.
- (32) Herzberg, G. *Molecular Spectra and Molecular Structure I*; van Nostrand Reinhold Co.: New York, 1950.
- (33) *NIST Chemistry WebBook, NIST Standard Reference Database Number 69*; Linstrom, P. J., Mallard, W. G., Eds.; July 2001, National Institute of Standards and Technology: Gaithersburg, MD (<http://webbook.nist.gov>).
- (34) Damin, A.; Dovesi, R.; Zecchina, A.; Ugliengo, P. *Surf. Sci.* **2001**, 479, 255.
- (35) Föhlisch, A.; Nyberg, M.; Hasselström, J.; Karis, O.; Pettersson, L. G. M.; Nilsson, A. *Phys. Rev. Lett.* **2000**, 85, 3309.
- (36) Bagus, P. S.; Hermann, K.; Bauschlicher, C. W., Jr. *J. Chem. Phys.* **1984**, 80, 4378. Bagus, P. S.; Hermann, K.; Bauschlicher, C. W. Jr., *J. Chem. Phys.* **1984**, 81, 1966. Bagus, P. S.; Illas, F. J. *J. Chem. Phys.* **1992**, 96, 8962.
- (37) Bredow, T.; Márquez, A. M.; Pacchioni, G. *Surf. Sci.* **1999**, 430, 137.
- (38) Di Valentin, C.; Pacchioni, G.; Bredow, T.; Dominguez-Ariza, D.; Illas, F. *Mol. Phys.* In press.
- (39) Bredow, T.; Geudtner, G.; Jug, K. *J. Comput. Chem.* **2001**, 22, 861.
- (40) Reinhardt, P.; Causà, M.; Marian, C. M.; Hess, B. A. *Phys. Rev. B* **1996**, 54, 14812.